Object-oriented and Decision tree classifications for LULC using Cosmo-SkyMed, QuickBird and LandSat 7 satellite data: An Example of Erbil/Iraq

Amjed AL-HAMEEDAWI [a,b], Manfred BUCHROITHNER [a] Nikolas PRECHTEL[a]

[a] Institute for Cartography, Dresden University of Technology, 01062 Dresden, Germany

[b]University of Technology, Baghdad

Abstract

Classification of SAR Data and optical remote sensing data is utilised in this paper to make use of complementary mapping potential of SAR data and optical image data. The landuse/landcover LU/LC mapping of the study area in Iraq has been performed using multi-sensor (SAR, optical) data in a combination with different classification approaches. The results have been evaluated on the basis of an accuracy assessment with a reference to substantial ground truth. The applied techniques include object-oriented classification and decision-tree classification. A good accuracy level has been reached. The results provide help and guidance for decision makers in an area with limited available geo-information.

The accuracy assessment of classification is not only dependent on which classification techniques used but also on image Pre-Processing techniques used. Therefore, a set digital image processing is made for SAR Data and Optical Remote Sensing Data. These pre-processing techniques were very important to increase features extracted from images, decrease error in interpretation of images and also in order to effectively identify the spatial distribution characteristics of landcover/landuse classes for the city of Erbil.

The Analysing and mapping the trend of LULC dynamics within the study area provide a basis for strategic planning, management and conservation decision making of Erbil City.

Keywords: Cosmo-SkyMed, LULC, Erbil

1 Introduction

1.1 Landuse / Landcover Classification

Classification is a process that associates image objects with a proper class. Through the process of classification, each image object is assigned to certain or uncertain class and thus linked to the class hierarchy. The output of the classification is a network of classified image objects with specific attributes, and specific relations to their objects in the class hierarchy. Image classification can be subdivided into supervised and unsupervised, or parametric and nonparametric, or hard and soft (fuzzy) classification, or per-pixel, sub-pixel, and per-field (Lu and Weng, 2007).

The parametric classifiers presume that a normally distributed dataset exists, and that the statistical parameters, reproduced from the training samples, are representative. In addition, deficient, non-representative, or multimodal distribution training samples can further introduce uncertainty to the image classification process.

Another major obstacle of the parametric classifiers results from the difficulty of integrating spectral data with ancillary data. With non-parametric classifiers, the presumption of a normal distribution of the dataset is not required (Mahmoud, 2012).

There is no need for statistical parameters in separation image classes. Consequently non-parametric classifiers are particularly proper for the conjunction of non-spectral data into a classification procedure (Lu and Weng, 2007). According to literature review as well as needs of study area, the main motivations of this paper can be shown as follows:

- Update data of study area shown in Figure 1 using two different classification methods.
- Update the data of study area to integrate with Master Plan of Erbil City up to 2030 and therefore provide the information necessary for decision makers
- Using new techniques including fused Cosmo-SkyMed image with Landsat 7 image and classification using Object-oriented methods (OOC).
- Using new techniques for Decision Tree Classification (DTC) on the basis of an QuickBird image, Normalized Difference Vegetation Index (NDVI) from Landsat 7, and information extracted from a digital terrian model (DTM) in desicion tree building.
- Comparing different classification methods (for optical and SAR data) according to accuracy assessment.
- This paper aims to map the LULC for study area using different classification methods and comparing the results.

The produced LULC maps within the study area will be used for documentation and analysis as a basis for strategic planning and management. Moreover this study provides help and guidance for making efficient and effective decisions by decision makers in Erbil City.

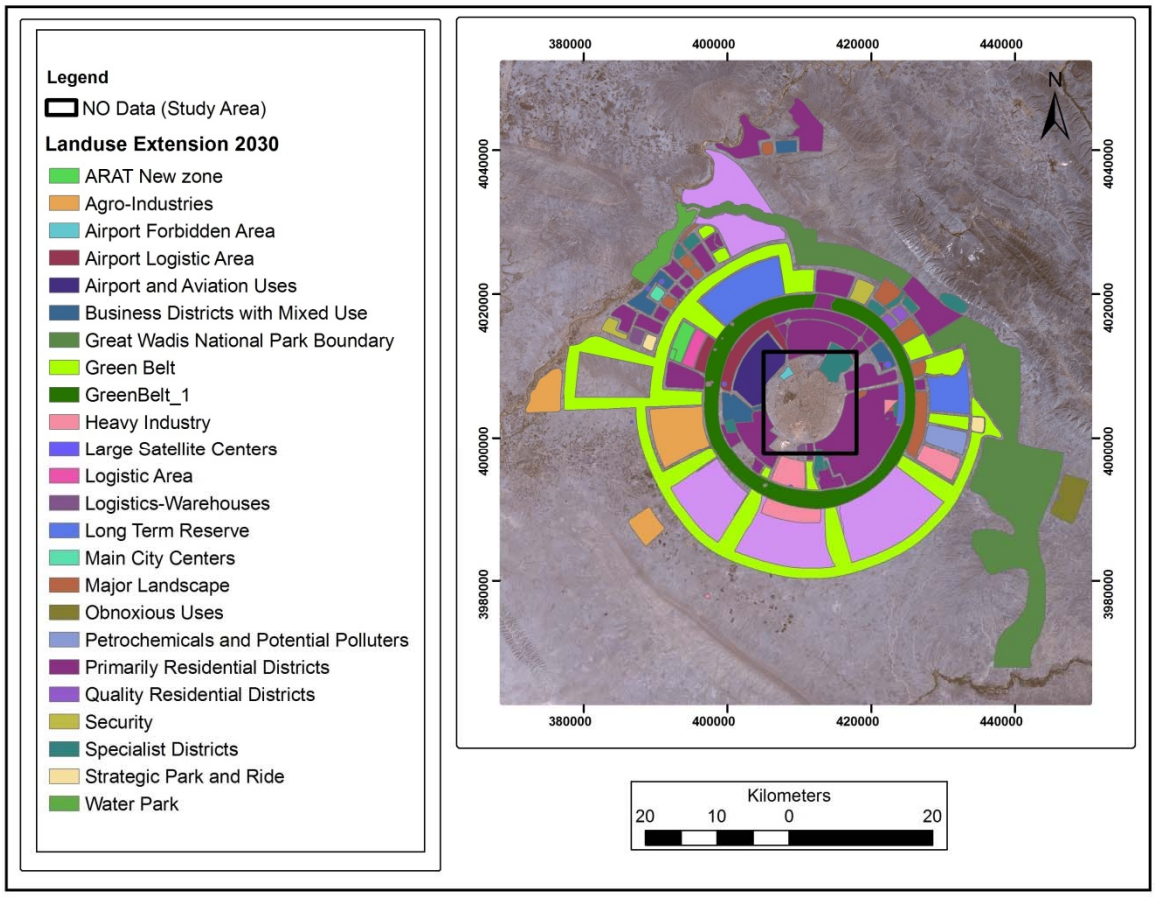

Figure 1: Map of Proposed Landuse according to Master Plan of Erbil City Up to 2030. Data Provided Courtesy of Erbil municipality, 2012.

1.2 Study Area

Erbil City is located in the north of Iraq. Erbil Province borders Turkey to the north and Iran to the east. Erbil composes with both Dahuk and Sulaymaniyah, the area run by the Kurdistan Regional Government (KRG). The City of Erbil is the capital of both Erbil Province and the KRG (OCHA and UNAMI, 2009). Mountains predominate the landscape towards the north east of the province; the relief in the southern part is rather plain, whilst the middle section is more undulated. Erbil City is located 316 km north of Bagdad and 80 km west of Mosul, and has road networks to Mosul to the west, Tikrit and Baghdad to the south-east, and the frontier of Iran to the north-west. Urban life at Erbil City can be dated back to at least 6000 B.C. and it is one of the oldest continuously inhabited cities in the

world. Erbil City was a major trading centre on the route between Baghdad and Mosul, a vital role that it still plays today with significant road networks to the outside world. The chosen study area is bounded by the coordinate from 405662.457926 m to 414992.977578 m easting and from 3999003.137635 m to 4009674.249192 m northing, in zone 38N according to UTM cartographic coordinate system (Fig. 1).

The population density of Erbil municipality and Erbil District is 135.5 (persons/km^2) and 472.9 (persons/km^2) respectively. Population growth in urban areas has a direct influence on the use of land, transportation, education, recreational, and places enormous need for housing and infrastructure (Bhaskaran et al., 2010).

1.3 Selection of Classification Approaches

Commonly, a classification approach is predetermined depending on the user's demands, spatial resolution of adopted remotely sensed data, consistency with the work, image-processing and classification algorithms attainable, and time restrictions. Such a system should be instructive, comprehensive, and separable (Jensen, 1996, Landgrebe, 2003***).*** Training samples are conventionally aggregated from fieldwork, or from fine spatial resolution aerial photographs and satellite images. Many factors, such as spatial resolution of the remotely sensed data, multifarious sources of data, a classification system, and obtainability of classification software must be considered when adopting a classification procedure for employment. Diversified classification procedures have their own virtues. The inquiry of which classification method is appropriate for a particular

study is not easy to determine. Disparate classification outcomes may be acquired depending on the classifier(s) chosen (Lu and Weng, 2007).

In this paper two classification methods have been used as follows:

1. Object oriented classification (OCC)

This type of classification method was selected for its procedure which enables users to encompass diversity of various details, ranging from spectral mean values for each object, to calculate of texture, context and shape (Herold and Scepan, 2002). Hence this type of classification give us the opportunity to make use of all image information in combinations with ground truth to help us accurately differentiate between different classes in the study area. Object-oriented classification is a modern and promising technology where textural and contextual/relational information is employed in addition to spectral information for classifying data.

2. Decision tree classification

Decision tree algorithm was adopted (Aksoy et al., 2004) for the following reasons: (1) it does not need a big portion of processing duration; (2) the model is effortlessly comprehended; (3) illustrative attributes are simply determined; (4) classification rules are uncomplicated, it does not necessitate assumptions about statistical distributions for classes; (5) object attributes can be delineated algebraically and categorically, and it has created advantageous consequences in Remote-sensing imagery classification (Pinho et al., 2008, Silva et al., 2008).

1.4 Fieldwork

The field study has taken place in Erbil City of Northern Iraq with a duration time of about eight weeks (in the Period 1st Dec.2011– 1st Feb.2012). The following activities are covered during the field work:

1- Surveying of the study site in order to obtain accurate location point data for each land-use/land-cover class within the research site using the Global Positioning System (GPS) instrument. This stage is often to be referred as the reference or ground truth data collection. Therefore one can be able to identify the land cover classes which appear in the satellite image.

2- Large numbers of potential landuse/landcover sites are investigated.

3- Data Collection : The data collected are divided into 2 following groups:

I) Primary Data are the surveying data of the study area.

II) Secondary Data are the collected data from the government office, in related field of the study.

The secondary data are consists of the following data:

- GIS Database: the GIS database about the natural resources and the environment of Erbil City.
- Various maps types with different scales.

2 Fundamentals

2.1 Object-oriented classification

Many significant advantages have been shown in Object-oriented classification (OOC) over other methods for classification of urban or forest ecosystems (Ouyang et al., 2011). The employment of available ancillary data, usually vector

information, along with imagery data in order to facilitate the process has been found in other studies (Bouziani et al., 2010, Doxani et al., 2012).

Both the spectral and the spatial information included in digital images are employed by Object-oriented classifications (OCC). The process of subdividing the image into groups of contiguous pixels, known as image objects or segments, corresponding to significative features or targets in the field, for instance road, house, water body, is called image segmentation.

The basic processing units of object-oriented image analysis are image objects and no single pixels (Benz et al., 2004, Mathieu et al., 2007). The scale factor is indirectly associated to the average size of the objects to be detected (it has no unit). It is an abstract expression which defines the peak permitted heterogeneity within an image object (Mathieu et al., 2007). There is a deep-rooted inclination to idealize landforms with no guarantee of consistency of landform and feature mapping between individual mappers (Saha et al., 2011).

Image classification is ordinarily used to obtain land-cover information from satellite images (Ouattara et al., 2004). Nowadays, as a result of availability of commercial high spatial resolution images, detailed features of the earth's surface can be found in the images, and consequently textural information. Therefore, the use of the traditional pixel-based classification methods is insufficient, because speed and accuracy is limited (Goetz et al., 2003). So as to make use of the spatial information facilities in the high spatial resolution images, it is necessary

that object-oriented analysis classifiers are utilized rather than pixel-based classifiers (Dean and Smith, 2003).

Gamanya et al., (2007) states that a strong and experienced evaluator of segmentation techniques is the human eye/brain combination. Many classification methods have been developed for classifying a remote sensing images; a comprehensive review of the same is given in Lu and Weng (2007).

The main idea related to the Ecognition software ("well-developed commercial one") is object-oriented. Multi-resolution segmentation method is an important algorithm in Ecognition. Scale parameter is an important parameter for image segmentation, which discerns the size of an image object.

The higher is the value of the scale parameter, the larger are the image objects (Wang and Niu, 2010). As per recommendation of the algorithm developers (Baatz and Schäpe, 2000), colour homogeneity was weighted more highly than shape homogeneity. Segmentation presumes that images are forming from regions, separated by edges, in which the radar reflectivity is stable.

The number and position of these segments and their mean values are unknown and have to be determined from the data. Rather than trying to reconstruct an estimate of the radar reflectivity for each pixel, segmentation seeks to overcome speckle by identifying regions of stable radar reflectivity (SARMAP, 2007).

2.2 Definitions *(Definiens, 2007)*

- *''Scale Parameter* is an abstract term which determines the maximum allowed heterogeneity for the resulting image objects. For heterogeneous data the resulting objects for a given scale parameter will be smaller than in more homogeneous data. By modifying the value in the Scale parameter value you can vary the size of image objects.
- *Colour and Shape:* by modify the shape criterion; you indirectly define the colour criteria. In effect, by decreasing the value assigned to the Shape field, you define to which percentage the spectral values of the image layers will contribute to the entire homogeneity criterion. This is weighted against the percentage of the shape homogeneity, which is defined in the Shape field. Changing the weight for the Shape criterion to 1 will result in objects more optimized for spatial homogeneity. However, the shape criterion cannot have a value more than 0.9, due to the obvious fact that without the spectral information of the image, the resulting objects would not be related to the spectral information at all.
- *Smoothness* is used to optimize image objects with regard to smoothness of borders. To give an example, the smoothness criterion should be used when working on very heterogeneous data to inhibit the objects from having frayed borders, while maintaining the ability to produce non-compact objects.
- *Compactness* is used to optimize image objects with regard to compactness. This criterion should be used when different image objects which are rather compact, but are separated from non-compact objects only by a relatively weak spectral contrast.

- *The grey level co-occurrence matrix (GLCM):* a tabulation of how often different combinations of pixel grey levels occur in an image. A different co-occurrence matrix exists for each spatial relationship. To receive directional invariance all 4 directions (0°, 45°, 90°, 135°) are summed before texture calculation. An angle of 0° represents the vertical direction, an angle of 90° the horizontal direction.
- *Mean:* Layer mean value is calculated from the layer values of all pixels forming an image object.
- *Maximum Difference (Max. diff.):* To calculate Max. Diff. the minimum mean value belonging to an object is subtracted from its maximum value. To get the maximum and minimum value the means of all layers belonging to an object are compared with each other. Subsequently the result is divided by the brightness''.

2.3 Decision Tree Classification (DTC)

Decision tree classification method has been successfully employed in an extensive range of classification issues, but only recently has it been tested in detail by the remote sensing community (Kandrika and Roy, 2008, Pal and Mather, 2003).

The classification framework determined by a decision tree is predestined from training data using a statistical procedure (Punia et al., 2011). A definition of a decision tree was given in Russell and Norvig (2002), as a production which 'takes as input an object or situation described by a set of merits, and outputs a yes/no decision. Decision trees subsequently represent Boolean functions'. The

integrations of these Boolean yes/no responses into a hierarchical ‘tree like’ structure composes the shape of a decision tree as it is commonly known (Aitkenhead, 2008).

The form a decision tree takes can commonly be clarified using the following statements (Aitkenhead, 2008):

- Classification occurs through continuing utilize of Boolean yes/no questions about particular attributes of the aspect.
- Attributes may be values (integers, floating-point, etc.) or features (on/off, characteristic kinds, etc.).
- Each inquiry, or parent node, has two daughter nodes which can either be parent nodes themselves or output nodes offering predictions.
- Output predictions are depicted by discrete classifications, denoting that the concept under argument is validated to be one thing or another.

2.4 Speckle

SAR is a consistent imaging technology that records both the amplitude and the phase of the back-scattered radiation (Lee and Jurkevich, 1990, Lee, 1986). The aim of the despeckling algorithm is to remove or reduce noise while, most of the image’s textural features. The most commonly employed despeckling filters are the Lee [1], Frost [2] and Gamma [3] filters (Lua et al., 2011). Bright or dark dots on the image will manifest, which represents the Speckle noises. This leads to a limitation on the accuracy of the measurements given that the brightness of a pixel is determined not only by properties (Gnanadurai et al., 2009). Speckle can be

reduced by special filtering and averaging techniques but cannot be completely removed (Buchroithner, 1993, Lillesand et al., 2008, Mahmoud, 2012).

2.5 Image Data Fusions

Data fusion approaches that fuse the details of dissimilar images will be incrementally influential to Geography for land-cover mapping. Various data fusion procedures, however, add spectral and spatial errors to the resultant data based on the geographical context; hence a careful choice of the fusion procedure is needed (Ashraf et al., 2012).

The procedure involved in radar imaging is quite different from that in VIS/IR imaging. These two sensor types give different information about the same target (chemical vs. physical), and they are complementary data sets. When the two images are correctly combined, the resultant image transfers both chemical and physical information and could prove more useful than either image alone. The methods for fusing or merging radar and VIS/IR data are still empirical and open for exploration (Erdas FieldGuide^{TM}, 2010).

Data fusion or merging of multi-sensor exploits heterogeneous image data for enhancement of visual interpretation and quantitative testing. In common, three categories of data fusion can be demonstrated (Gong, 1994) as follows: pixel (Luo and Kay, 1989), feature (Jimenez et al., 1999), and decision (Benediktsson and Kanellopoulos, 1999).

Data fusion encompasses two major steps: (1) geometrical co-registration of two datasets and (2) combination of spectral and spatial details to create a new dataset that accommodates the enriched details from both datasets.

2.5.1 Data Fusion Techniques Used

2.5.1.1 Brovey Transformation (BT)

Brovey Transformation (BT), as developed by R. L. Brovey, is one of the most broadly applied procedures and is relatively easy to use and advantageous (Li et al., 2007). It has restrictions because it employs only three bands, and also leads to color distortion (Dong et al., 2009). The BT was expanded to visually broaden contrast in the low and high ends of the image histogram and for creating visually appealing images (ERDAS, 2009, Ashraf et al., 2012). The formula for the BT is:

HRMI = (LRMI * HRPI)/ LRPI

Where: HRMI is a high resolution multi-spectral image, LRMI is a low-resolution multi-spectral image, HRPI is a high resolution panchromatic image, LRPI is a low resolution panchromatic image derived from the sum of any three LRMI bands.

2.5.1.2 Principal Component Substitution (PCS)

With principal component substitution (PCS), the LRMIs are converted to the principal component (PC) images according to the eigenvectors of their relating covariance matrices. The first PC (PC1) image is alternated by the HRPI. Prior to its exchange, the HRPI is algebraically corrected to match with the PC1 through two commonly applied procedures e the min-max stretch procedure, and the mean

and variance stretch procedure. The fused images are gotten by applying an inverse transformation on the fresh category of components (Cetin and Musaoglu, 2009, Chavez et al., 1991, Shettigara, 1992, Wang et al., 2005).

3 Preparations of Remote Sensing Data

3.1 Optical Data

QuickBird image acquired on 5.4.2011 offers panchromatic and multi-spectral imagery with the highest spatial resolution currently available within the satellite sensors. Landsat 7 Image was obtained from USGS (http://glovis.usgs.gov/), which is the image acquired on 3.5.2011.

Optical remote sensing data were used in order to effectively identify the spatial distribution characteristics of land cover / land use classes for the city of Erbil. By using ENVI software, the images were radiometrically corrected and enhanced using relative correction and enhancement method (histogram equalization), to facilitate the information extracted from the images. The Landsat 7 is used to extract Normalized difference vegetation index (NDVI) which has been found to be a good indicator for vegetation cover.

3.2 SAR Data

Two Cosmo-SkyMed images were acquired in the Spotlight-Ping-Pong mode with two polarisations HH and VV on 07.06.2011. The SAR Data used in this study is Cosmo-SkyMed (images acquired on 6 July 2011) with two polarisations HH and VV. They were rectified, enhanced (in addition to remove speckle) and segmented

and then classified according to Object-oriented classification method. The two SAR images were geocoded.

Synthetic Aperture Radar (SAR) geocoding is generally known as the procedure of implementing geometric transformation of SAR imagery with the help of a digital elevation model (DEM) from the original radar azimuth/range coordinate system to map projection coordinate systems (Zhang et al., 2012). Terrain Geocoding and radiometric calibration has been processed using SARscape software. The Cosmo-SkyMed Image is imported and converted to single-look complex (SLC) SAR image product.

The information regarding primary modes of image acquisition Cosmo-SkyMed can be found in a file name. The geometric correction must consider the sensor and processor characteristics and thus must be based on a strict range-Doppler approach. A high precision geocoding of the image information helps in removal of geometric distortions (SARMAP, 2007).

Figure 2 represents the general methodological framework for this study.

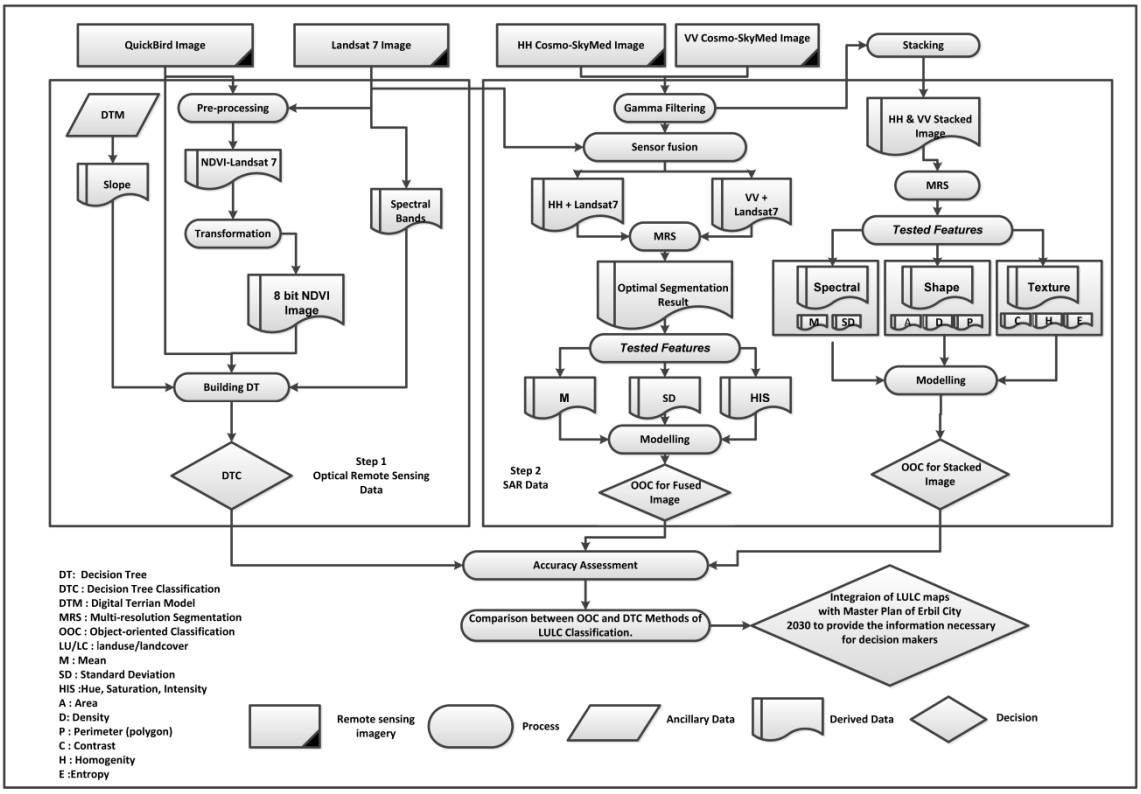

Figure 2: Flow Chart of General Methodological Framework.

4 Methodology

4.1 Speckle Filtering

4.1.1 Speckle Reductions

For this purpose, two images are presented - one that has been despeckled, and one raw SAR image. The IMAGINE Radar Interpreter module Speckle Suppression filters have been prepared to be versatile and gentle in decreasing noise (and also resolution). The coefficient of variation for an image is calculated too. This variable is necessary in order to fine-tune many Speckle Suppression filters. When processing radar imagery, it is feasible to use the Speckle

Suppression functions before other image processing functions to avert incorporating speckle into the image (ERDAS Field Guide™, 2010).

4.1.2 Speckle Suppression Index (SSI)

After performing Speckle Suppression Function three adaptive speckle filters, specifically, Enhanced Lee, Enhanced Frost (Lopes et al., 1990) and Gamma (Lopes et al., 1993) were performed to Cosmo-SkyMed images with kernel sizes of 3x3, 5x5 and 7x7 respectively. These locally adaptive speckle filters smoothen out the speckle in the homogeneous area while preserving textures and high-frequency information in the heterogeneous areas. Speckle Suppression Index (SSI) is used to identify a proper filter algorithm. This index is inclined to be less than 1 if the filter efficiency is adequate in reducing speckle noise (Biro, 2011, Sheng and Xia, 1996). In addition, the lower standard deviation (Std) value might be a good point for a suitable adaptive algorithm. The SSI is based on the following equation:

$$SSI = \frac{\sqrt{\mathbf{Variance(If)}}}{\mathbf{Mean(If)}} x \frac{Mean\ (Io)}{\sqrt{\mathbf{Variance(Io)}}} \qquad \textbf{[1]}$$

Where:

(If) is the filtered image

(Io) is the noisy image.

4.2 Image Data Fusions

In this section were fused Cosmo-SkyMed with Landsat 7 in two different methods include BT transformation and PCS then results are compared according to quantitative techniques as follows: First it was fused HH Cosmo-SkyMed with the Landsat 7 where we used Bands 4, 5 and 6, which are thermal because of their usefulness to separate vegetation and landcover classes from others besides BT has restrictions that only three bands can be applied so as to compare the results inputs must be identical for both methods to compare. In the same way we can fuse VV Cosmo-SkyMed with the Landsat 7 and determine which polarization give better results according to quantitative techniques.

4.2.1 Evaluation of Fusion Technique

*A quantitative technique is essential to utilize both Spectral and spatial metrics (Gangkofner et al., 2008). These incline to demonstrate opposite inclinations and discern the trade-off between the spatial and spectral details of the fusion outputs (*Ashraf, 2012*). To measure spectral details, root-mean squared error (RMSE) is used. To measure spatial details, the RMSE of edge detector filtered images are used.*

3 x 3 Edge detect filter is as follows:

-1	*-1*	*-1*
-1	*8*	*-1*
-1	*-1*	*-1*

The Root Mean Squared Error (RMSE) measures the standard error between the LRMI and the resultant HRMI (Gangkofner et al., 2008, Li et al., 2010, Pradhan, et

al., 2006). The RMSE can effectively distinguish the similarity between LRMI and resultant fused HRMI (Gangkofner et al., 2008).

Aschraf et al., 2012 has used Sobel filter (which is edge detect filter) to measure spatial details after the fusion process is carried out. In order to measure spatial details we have used filter based RMSE is a quantitative method for comparing the edge magnitude difference of the LRMI and resultant HRMI. The filter measures the edge intensities.

4.3 Object-oriented Classification (OOC)

In this paper particular image objects associated to the various classes were created repetitively in Definiens eCognition software by applying the multi-resolution segmentation procedure. The accuracy of the classification is directly affected by the segments (Bhaskaran et al., 2010). A lot of parameters were used such as shape, compactness, and scale parameters for each of Cosmo-SkyMed image and fused image where HH and VV polarizations of Cosmo-SkyMed image were stacked then used in the extraction of a wide range and size of urban features. In fused image which is combination of Landsat 7 and Cosmo-SkyMed the following procedure is carried out: Cosmo-SkyMed polarizations were fused with specific bands of Landsat7 as illustrated in Table 4 and 5 where a lot of iteration has been made until we reached to the best result. The accuracy of these segments was checked with ground truth proved image that was devised from a combination of fieldwork surveying.

The software used in this research, eCognition V7.0, uses a multi-resolution segmentation approach which is basically a bottom-up region-merging technique starting with one-pixel objects (Section 2.1). Object-based classification is a different technique and is dependent on the classification of image objects which have resulted from previous segmentation applied to a remote sensing imagery (Petropoulos et al., 2012).

4.4 Segmentation Algorithms

The segmentation process applies by accepting the mutual-best fitting basis and the fundamental concept is the segmentation process begins with single image objects of 1pixel size and merges them to bigger units until an upper threshold of homogeneity is exceeded locally. The seed looks for a feasible merger by its best-fitting adjacent object (Fig.3a) when best-fitting is not mutual; the best adjacent object fits the up-to-date seed to detect its best-fitting partner, which is shown in Figure 3 b (according to Ecognition).

This process repeats until mutual-best fitting partners are detected (Fig.3c) (according to Ecognition). When best-fitting is mutual and the homogeneity of the new image object does not exceed the scale parameter, the two partner image objects are merged, (Fig.3d) (according to Ecognition).

In each loop, each image object is handled once. The process keeps continuing with another image object's best adjacent object. The steps repeats until no further image object can be merged without exceeding the maximum envisaged homogeneity of an image object (according to Ecognition, Wang and Niu, 2010).

We adopted multi-resolution segmentation for two justifications which included, firstly, the study area has an expansive extent of various object dimensions, these objects may be connected with diversified scales of portrayal, paralleling to a sort of details that can include different sizes from small objects to large objects hence this type of segmentation is flexible to deal with different object dimensions. The second stimulus was the conceivability of determining disparate weights for shape and spectral details in the segmentation process.

The tested features used for a Cosmo-SkyMed Image fused with Landsat 7 scene of the Erbil City (Iraq) are listed in Table 1 and Figure 4. In Table 2 and Figure 5 the tested features for Cosmo-SkyMed Image can be seen.

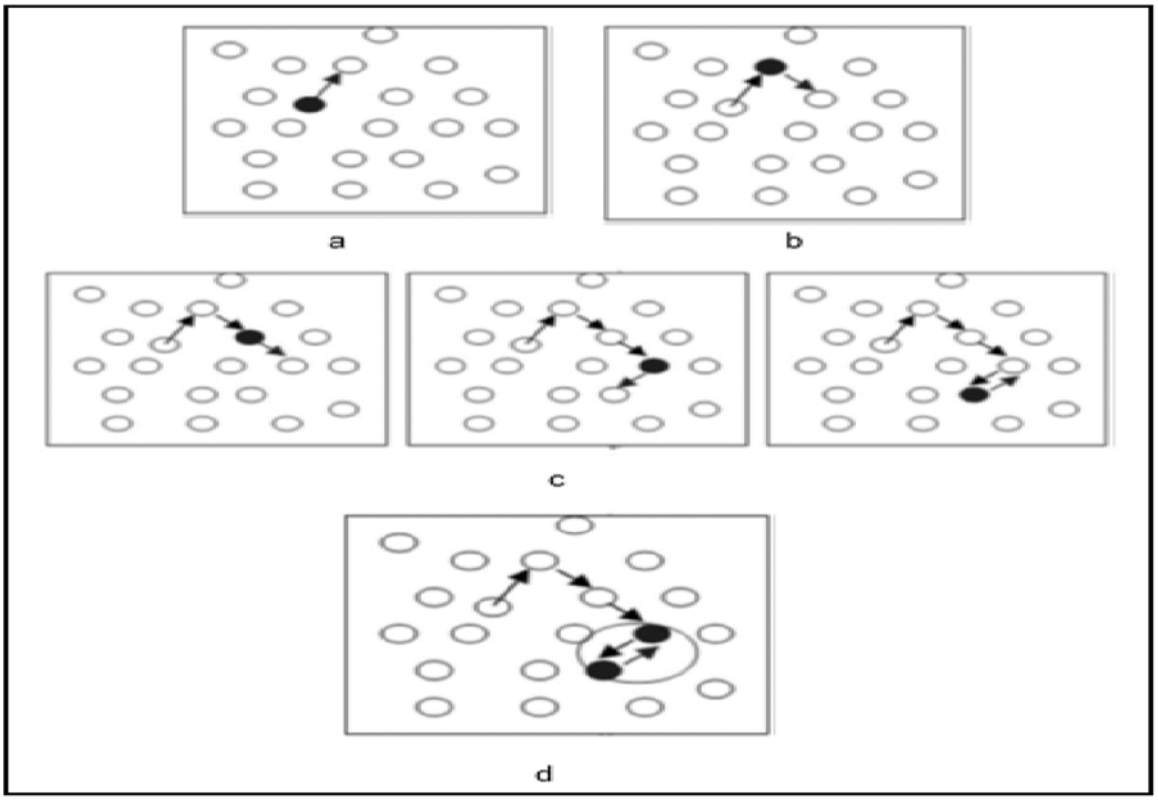

Figure 3: a) Searching for the best adjacent object to merge with by the homogeneity criterion, b) Stirring to the second object to find the best adjacent object, c) Iterating until mutual -best fitting partners are detected and d) The two mutual-best fitting partners are merged (Wang and Niu, 2010).

Table 1: List of the tested features for a Cosmo-SkyMed Image fused with Landsat7 scene of the Erbil City (Iraq) the two Images acquired on 2011.

Features	**Descriptions**
Mean	Maximum difference (Max. diff.) for three layers
Standard Deviation	Layer 1, layer 2 and layer 3
(HIS Transformation) Hue, Saturation, Intensity	Hue(R= Layer 1, G=, layer 2, B= layer 3). output (Hue, Saturation, Intensity)

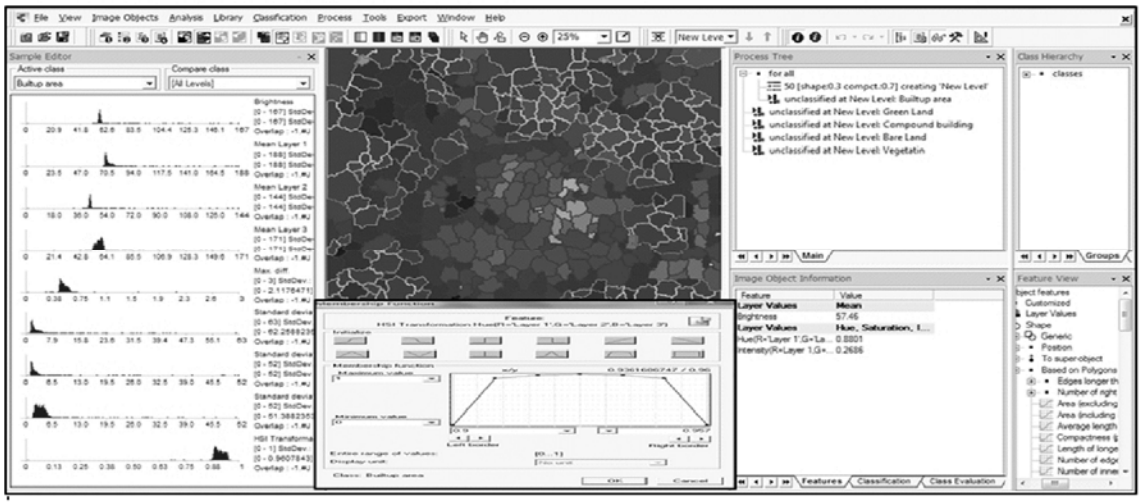

Figure 4: Tested Features and Sample Editors for a Cosmo-SkyMed Image fused with Landsat7 Image.

Table 2: List of the Tested Features for a Cosmo-SkyMed Data Classification.

Features	**Descriptions**
Spectral: 1. Mean 2. Standard Deviation	 Maximum difference (Max. diff.) for two layers Layer 1 and layer 2[1]
Shape: 1. Area 2. Density 3. Perimeter (polygon)	 Generic Generic based on polygon
Texture (after Haralick): 1. Contrast 2. Homogeneity 3. Entropy	 GLMC[2] layer 1 & layer 2 GLCM layer 1 & layer 2 GLMC 0 direction, layer 1 & layer 2
1 layer 1 = HH polarization & layer 2 = VV polarization; 2 GLCM = Grey-Level Co- Occurrence Matrix	

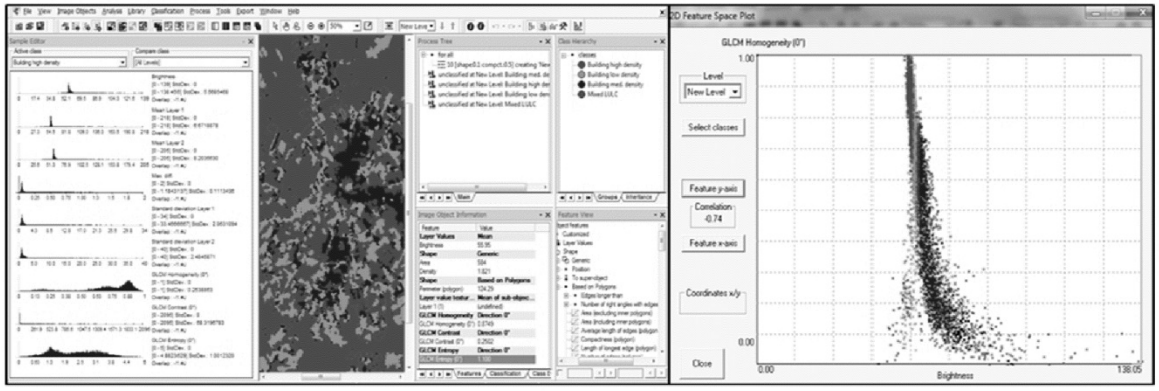

Figure 5: Tested Features, Sample Editors and 2D Feature Space Plot for a Cosmo-SkyMed Image.

4.5 Decision Tree Classification

This decision is based on the following dataset digital terrain models where this used to extract slope parameter for study area. Satellite images (QuickBird 2011) were obtained free of charge from the Ministry of Municipalities of the Kurdistan Regional Government. The derived NDVI Image from Landsat 7 helps to determine decisions in the tree. QuickBird image was used in order to effectively identify the spatial distribution characteristics of land cover / land use classes for the city of Erbil using ENVI software.

NDVI image was calculated using Landsat 7 acquired on (2011). The original NDVI had the values between -1 to +1, but they were transformed into image of 8 bit (0-255) value. The resultant NDVI image was correlated with the land use/cover classes, and the relationship between them analyzed. NDVI-Digital values have been used in decision tree inputs.

4.6 Accuracy Assessment

Accuracy assessment of landuse/landcover classification represents a great dilemma to classification outcomes. To evaluate the classification accuracy, independent ground truths aggregated during the fieldwork, high resolution images and other set of landuse/landcover maps have been employed for this purpose.

The GPS points (200 points) were randomly dispersed all over study area for each classification method. Moreover samples (vector) of classes were exported from Definiens eCognition software and positioned on the QuickBird image.

A ground truth class image was produced by using the vector samples aggregated from the field and by transforming to a raster format. Hence it can be compared between authentic classes and resultant classes from classification. A set of landuse/landcover data gathered and grouped during the fieldwork of existing activity was also kept separate for accuracy assessment.

The landuse/landcover type's data of these places (GPS points) was compared with classification outcomes. The field samples were positioned on classification outcomes to assess intended classes. The matrix bestowed the correspondence between the envisioned and the authentic classes of membership for an independent checking dataset. This made it achievable to derive a range of quantitative calculations of classification accuracy. Producers, users, and overall accuracy were calculated to evaluate the accuracies of the classification results. An algorithmically valid sampling agenda was chosen to assess overall accuracy (Joshi et al., 2006, Stehman, 1996).

5 Results and Discussion

5.1 Image Filtering

After run speckle suppression model using Lee-Sigma filter and Local Region respectively, the results are shown in Table 3. The Model is repeated until the histogram of the image shows no more spikes (ERDAS Field Guide™, 2010).

Table 3: Speckle Suppression Parameters of Cosmo-SkyMed Image.

Pass	*Input file*	*Output file*	*Coef.of Var.*	*Coef. Of Var.Multiplier*	*Kernel Size*
1	Cosmo-SkyMed Image	Despeckle1	0.235346	0.5	3 × 3
2	Despeckle1	Despeckle2	0.188045	1	5 × 5
3	Despeckle2	Despeckle3	0.135025	2	7 × 7

5.1.1 Speckle Suppression Index (SSI)

After computing Speckle Suppression Index (SSI) for Enhanced Lee, Enhanced Frost and Gamma filter the best one will be selected (lower SSI value). Figure 6 show that the Gamma filter with kernel size 7x7 yielded the best results with lower SSI value of 0.786. According to Biro (2011) and Maged (2001) the Gamma algorithm not only provides very high speckle reduction but also preserves the spatial resolution. In addition, textural properties of the SAR data were much better preserved by using Gamma filter (Biro, 2011, Nezry et al., 1995).

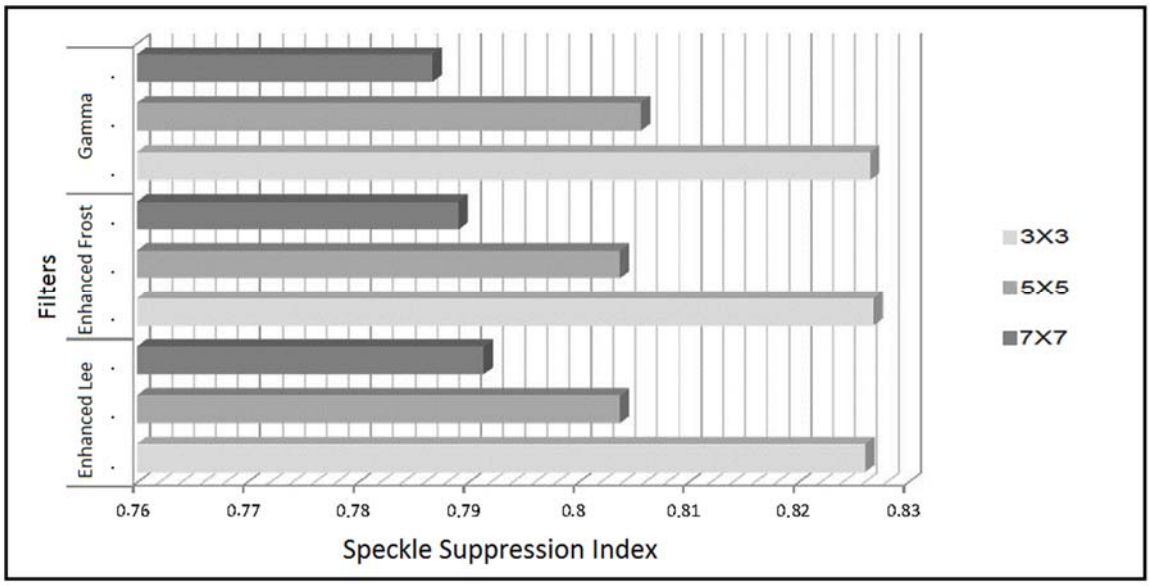

Figure 6: Speckle Suppression Index (SSI) values for each adaptive filter tested for Cosmo-SkyMed Image.

5.2 Gamma Filtering

Gamma Filter with Kernel Size 7x7 will be implemented on original noisy image and image derived from the speckle suppression function and then the results are compared according to Speckle Suppression Index (SSI). It is obvious from Figure 7 that the best result is obtained when the Gama filter is implemented after running Speckle Suppression Function because of the lower value of Speckle Suppression Index.

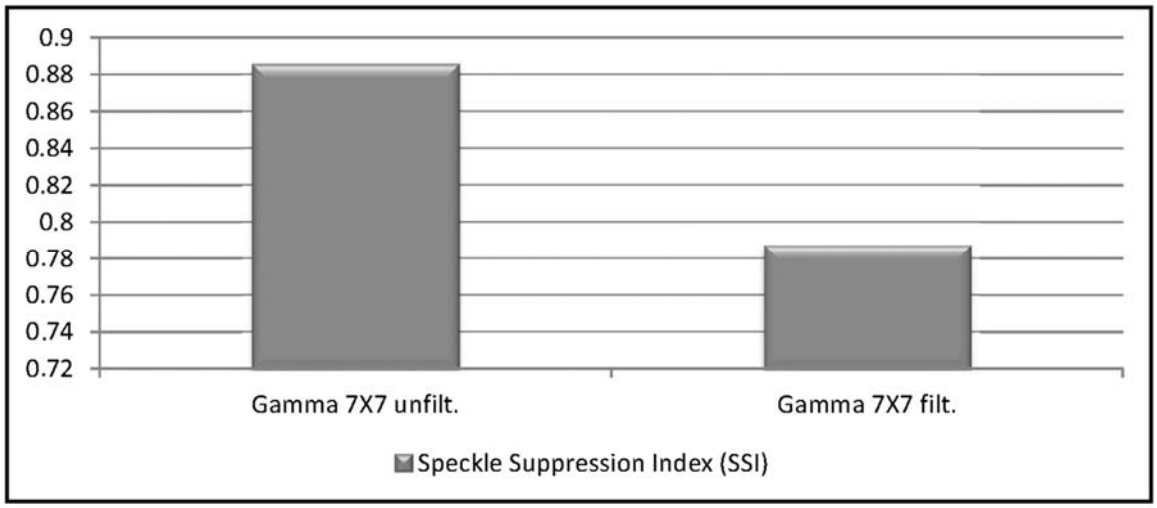

Figure 7: Speckle Suppression Index (SSI) values for comparing the Results for Gamma 7X7 for Image derived from the speckle suppression Function and Gamma 7X7 for Image derived from original noisy Image.

5.3 Image Data Fusion

The most conventional procedure to compare data fused techniques is qualitative evaluation by visual examination; although, it is subjective and based on many elements combining (1) showing images at coherent scale, (2) coherent data stretching, (3) applying identical band combinations, and (4) efficiency of graphic display.

Quantitative comparisons bestow a more objective evaluation of both the spatial sharpening and spectral fidelity (Ashraf et al., 2012). Hence Figure 8 is displayed using the same colour lookup values, coherent scale and care for consistency.

PCS technique show not only less colour distortion but also less spatial detail distortion than BT technique for both polarizations of Cosmo-SkyMed Fused with Landsat7. When compare PCS between HH and VV polarizations we can conclude they have the same spatial details effects but in spectral details, when HH polarisation of Cosmo- SkyMed fused with Landsat 7, it has gained better results than VV polarisation. Please see Tables 4 and 5.

Table 4: Evaluation of Spectral and Spatial Details Using Quantitative Technique for Landsat 7 Satellite Image Fused with HH Cosmo-SkyMed.

Fusion Techniques	*Spectral measure between LRMI and resulted HRMI bands*				*Spatial measure between LRMI and resulted HRMI bands*			
	Spectral RMSE				*Edge detect Filter RMSE*			
	Band4	*Band5*	*Band 6*	*Average*	*Band4*	*Band5*	*Band6*	*Average*
PCS	**65.5**	145.2	**12.856**	**74.51867**	**10.413**	**17.27**	**1.297**	**9.66**
BT	223.526	**106.178**	15.351	115.0183	10.769	17.619	1.47	9.9526

Hint: Best results are shown as bold values.

Table 5: Evaluation of Spectral and Spatial Details Using Quantitative Technique for Landsat 7 Satellite Image Fused with VV Cosmo-SkyMed.

Fusion Techniques	*Spectral measure between LRMI and resulted HRMI bands*				*Spatial measure between LRMI and resulted HRMI bands*			
	Spectral RMSE				*Edge detect Filter RMSE*			
	Band4	*Band5*	*Band 6*	*Average*	*Band4*	*Band5*	*Band6*	*Average*
PCS	**65.644**	145.469	**12.879**	**74.664**	**10.413**	**17.27**	**1.297**	**9.66**
BT	140.187	**40.014**	57.62	79.273	10.687	17.546	1.298	9.843

Hint: Best results are shown as bold values.

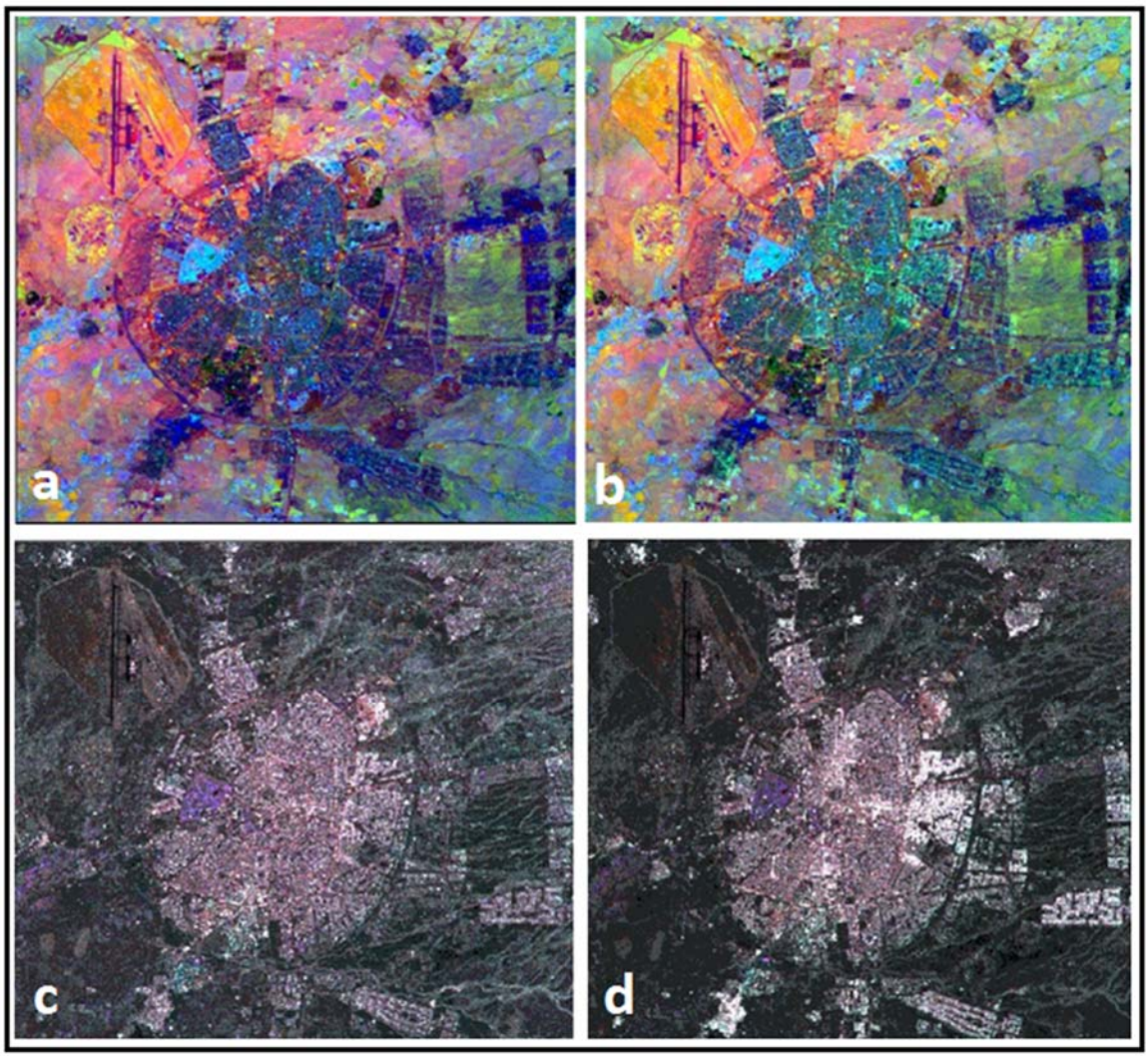

Figure 8 : fused images, ***a)*** *fused image (VV Cosmo-SkyMed plus LandSat7) from PCS method,* ***b)*** *fused image (HH Cosmo-SkyMed plus LandSat7) from PCS method,* ***c)*** *fused image (VV Cosmo-SkyMed plus LandSat7) from BT method, and* ***d)*** *fused image (HH Cosmo-SkyMed plus LandSat7) from BT method.*

5.4 Multi-resolution Segmentation

Figure 9a and b below shows the segmentation images achieved at two scales, namely with 10 and 50 respectively. The parameters used in multi-resolution segmentation are: scale, colour (spectral criteria), and shape (including smoothness and compactness).

Navulur (2007) states that for heterogeneous data the resulting objects for a given scale parameter will be smaller than in most homogeneous data.

Tested segmentation parameters were 10 Scale Parameter, 0.1 Shape and 0.5 Compactness for Cosmo-SkyMed (resolution 10.664345 m).

These parameters are repeated until the best result of segmentation is reached. In Figure 9a, on the other hand, tested segmentation parameters were 50 Scale Parameter, 0.3 Shape and 0.7 Compactness for fused Image (resolution 20m). Also the parameters are repeated until the best result of segmentation is reached (Fig.9b), it can be concluded there is a relationship between spatial resolution and scale parameter (Tab. 6).

Table 6: Tested Segmentation Parameters.

Data	Tested Parameters	Spatial Resolution (m)
Cosmo-SkyMed HH & VV	10 Scale Parameter, 0.1 Shape and 0.5 Compactness	10.664345
Fused Image	50 Scale Parameter, 0.3 Shape and 0.7 Compactness	20

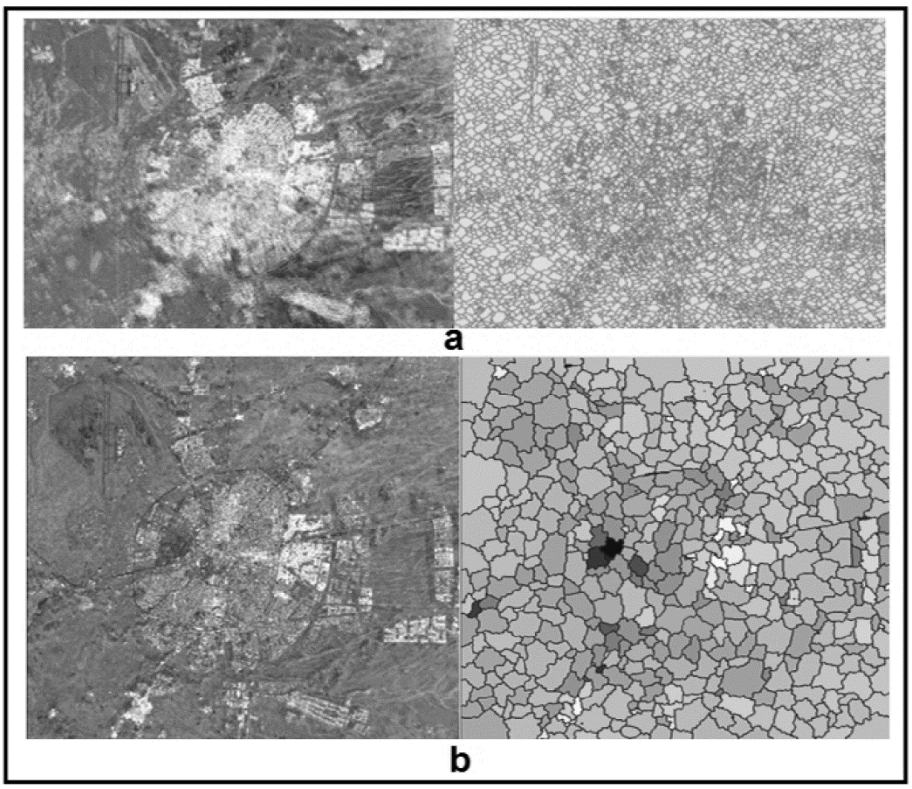

Figure 9: Multi-resolution Segmentation a) 10 Scale Parameter, 0.1 Shape and 0.5 Compactness of Cosmo-SkyMed and b) 50 Scale Parameter, 0.3 Shape and 0.7 Compactness of Fused Image.

5.5 Implementing of Object-oriented Classification (OOC)

Figure 10 below illustrates a scene generated by a Fusing of Cosmo-SkyMed and Landsat scene of Erbil City (Section 2.5). The two Images were acquired on 2011. Once a suitable segmentation was found, image objects were classified by membership functions. The features were calculated based on image segmentation. The object-oriented method possesses much more compact knowledge representation, higher efficiency, more continuous classifying result and higher prediction accuracy compared with other classification methods. The parameters used of Fused Image are 50 Scale Parameter, Shape/Compactness (0.3/ 0.7). Table 7 represents classification key for study area.

Table 7: Classification Key

Classes	*Description*
Built-up area	''Urban or Built-up Land is included with areas of intensive use with much of the land covered by structures. Included in this category are cities, towns, villages, strip developments along highways, transportation, power, and communications facilities, and areas such as those occupied by mills, shopping centres, industrial and commercial complexes, and institutions that may, in some instances, be isolated from urban areas'' (Anderson et al., 1976).
Vegetation	Including different trees types and greenbelt in Erbil City.
Compound Building	Building that composed of a number of parts in Erbil City.
Green Land	Including gardens and parks in Erbil City.
Barren Land	''Barren Land is land of limited ability to support life. In general; it is an area of thin soil, sand, or rocks. Vegetation, if present, is more widely spaced and scrubby (Anderson et al., 1976)''. These areas in accordance with the Master Plan of Erbil City 2030 will be converted to different uses of the land where these spaces represent the intersection between the proposed expansion and the study area.

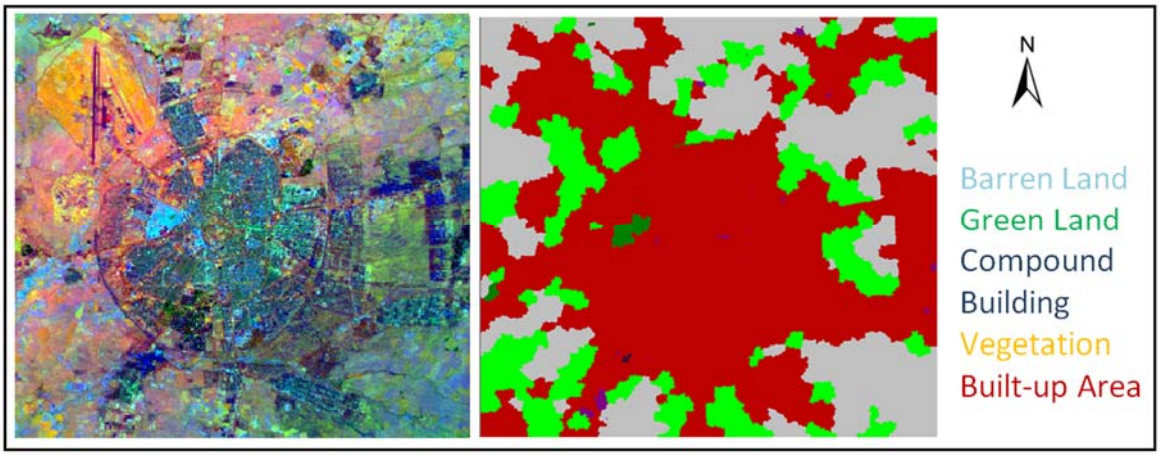

Figure 10: Object-oriented Classification of Fused Image.

Figure 11 below illustrates a Cosmo-SkyMed scene of the Erbil City (Iraq) acquired on July 6th 2011. The parameters used to classify Cosmo-SkyMed image (stacked) are 10 Scale Parameter, 0.1 Shape and 0.5 Compactness of Cosmo-SkyMed. This classification made use of old shape files to the Erbil City and different map types with different scales and the resulting classification.

Overall classification accuracy of Cosmo-SkyMed and fused Image according to object-oriented classification is 86.50%, and 92% respectively.

The reference data was obtained from surveying of the study site. In order to obtain an accurate location, a point data for each land-use/land-cover class within the research site is obtained using the Global Positioning System (GPS) instrument.

This stage is often to be referred as the reference or ground truth data collection. Where land cover classes can be identified by using recent remote sensing data, old shape files to the study site and various maps types with different scales have been used. Moreover, point data has been gathered using global position system (GPS) for this purpose (Section 4.6). Classes were mapped in the field: built-up area, vegetation, compound building, green land and barren land (Tab. 7).

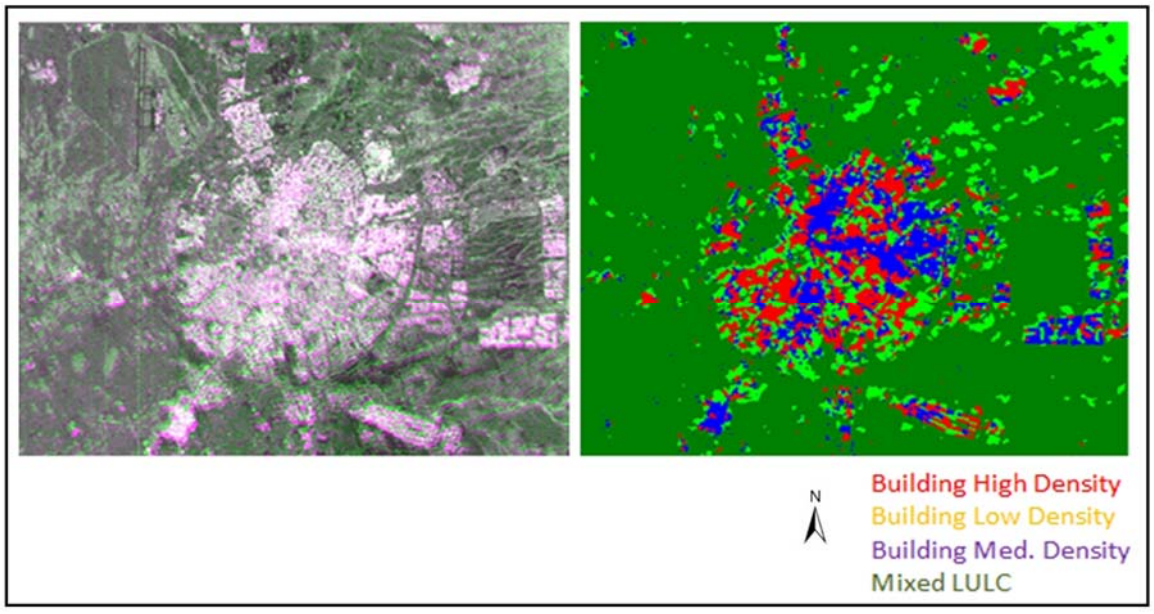

Figure 11: Object-oriented Classification of Cosmo-SkyMed (Stacked) _ Erbil City.

5.6 *Decision Tree Classification (DTC)*

This decision is based on the following dataset: a digital terrain model (DTM), satellite image (QuickBird 2011) and derived NDVI Image from Landsat 7. Those images contribute to decisions within this tree. NDVI image was computed using Landsat 7 acquired on 2011.

The original NDVI had the values between -1 to +1, but we transformed NDVI values into image of 8 bit (0-255) value. The resultant NDVI image was correlated with the land use/cover classes, and the relationship between them examined. NDVI-Digital values have been used in decision tree input. The average NDVI value for each land cover patterns then is found and given in Table 8.

Table 8: The digital value of NDVI per landuse/ landcover classes (LULC).

Class No.	LULC Classes	NDVI- Digital Values have been used in Decision Tree Input
1	Green Land	199
2	Urban	74
3	Bare	92
4	Other	82
5	Vegetation	156

The number of classes must be limited, but, at the same time, the total range of land cover or land use of a large territory has to fit into the system (Prechtel, 2000). Figure 12 represents the result of applying Decision Tree Classification for QuickBird image acquired on 2011. The Overall Classification Accuracy and Overall Kappa Statistics were 88.28%, 0.8119 respectively.

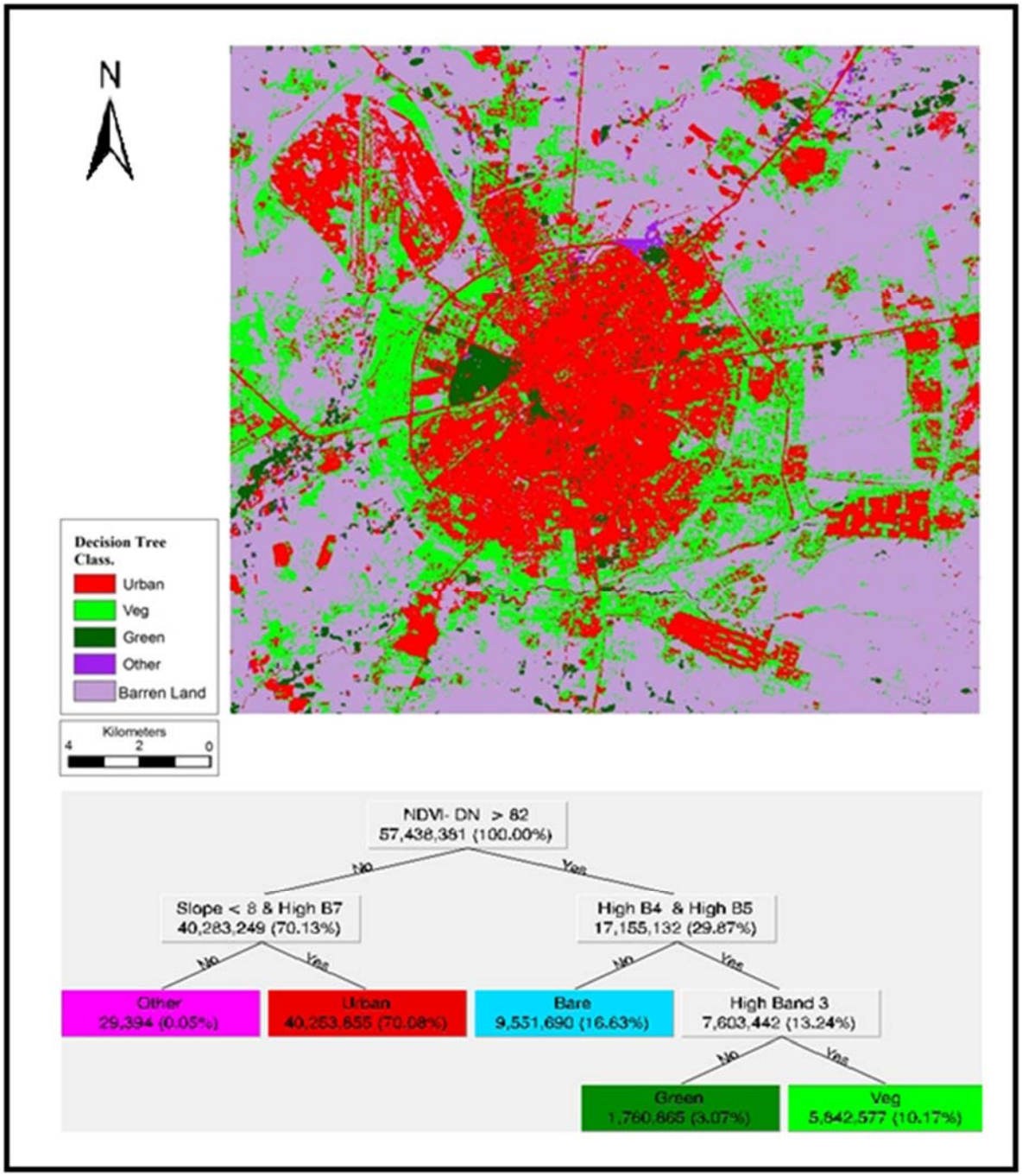

Figure 12: Decision Tree Classification of QuickBird Image.

5.7 Accuracy Assessment

The error matrix is one of the most popular tools employed in classification accuracy assessment. Error matrices compare the relationship between known reference data and the corresponding results of an automated classification. Such matrices are square, with the number of rows and columns identical to the number of classes whose classification accuracy is being assessed. The error matrix is used to derive other important accuracy assessment items such as overall accuracy, omission error, commission error, and kappa coefficient (Lillesand et al., 2008, Lu and Weng, 2007). By using tested map for Erbil city combined with GPS measurements, the classification was evaluated (Section 4.6). A total number of 200 random points were sampled, two classifications were evaluated (Fig.13). The accuracy measures were computed and analysed from the errors matrices (Tab. 9 - 11).

Table 9: Error Matrix and Overall Accuracy for OOC of Fused Image.

Classified data	Reference data						User acc. (%)
	Unclass.	Bare Land	Green Land	Compound Building	Veg.	Built –up Area	
Unclass.	0	0	0	0	0	0	-
Barren Land	0	9	0	0	0	0	100%
Green Land	0	3	52	0	0	2	91.23%
Compound Building	0	1	2	96	3	1	93.20%
Veg.	0	0	0	0	3	0	100%
Built-up Area	0	0	1	1	2	24	85.71%
Producer acc. (%)	-	69.23%	94.55%	98.97%	37.50 %	88.89%	-
Overall Classification Accuracy = 92.00% Overall Kappa Statistics = 0.8768							

Table 10: Error matrix and user's, producer's and overall accuracy, and Kappa Statistics for Decision Tree Classification (DTC).

Class. data	Reference data					User acc. (%)
	Urban	Veg	Green	Other	Bare	
Urban	62	3	2	3	2	86.11%
Veg	2	33	3	3	0	80.49%
Green	0	0	3	0	0	100 %
Other.	0	0	0	0	0	-
Barren Land	3	4	3	2	128	91.43%
Produc. acc. (%)	92.54%	82.50%	27.27%	-	98.46%	-
Overall Classification Accuracy = 88.28% Overall Kappa Statistics = 0.8119						

Table 11: Error Matrix and Overall Accuracy for OOC of Cosmo-SkyMed Image (Stacked HH & VV).

Classified data	Reference data				User acc. (%)
	Building High Density	Building Low Density	Building Med. Density	Mixed LULC	
Building High Density	89	3	3	5	89.00%
Building Low Density	1	12	2	0	80.00%
Building Med. Density	0	0	26	4	86.67%
Mixed LULC	2	0	7	46	83.64%
Producer acc. (%)	96.74%	80.00%	68.42%	83.64%	-
Overall Classification Accuracy = 86.50%, Overall Kappa Statistics = 0.7955					

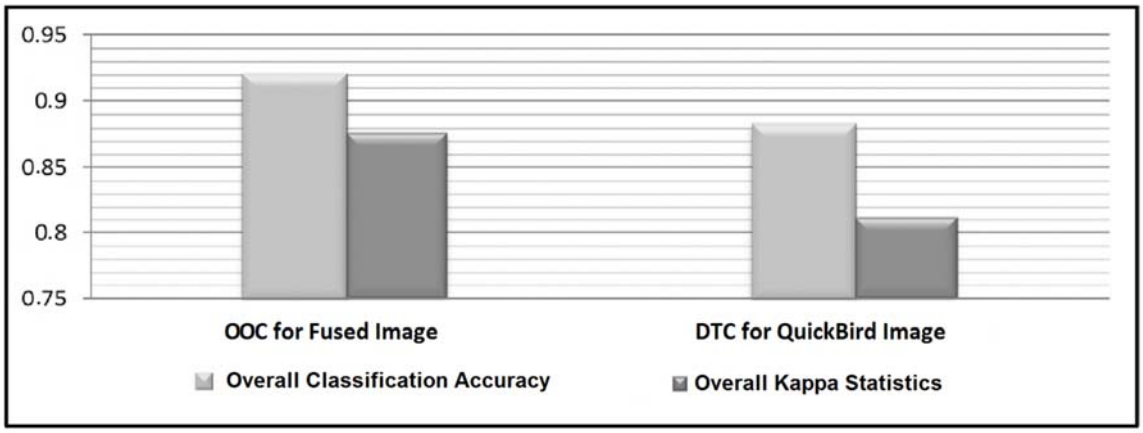

Figure 13: Comparison between OOC and DTC Methods of LULC Classification.

6 Conclusions

There is no classification method which can ideally map the reality which all researchers look for nor can meet all needs for mapping landscape due to limitations in all classification methods in addition to uncertainty in data. Therefore in this paper we have adopted specific classification methods based on image enhancements, speckle reductions and image fusion techniques by which classification can be upgraded to high accuracy close to the truth and appropriate for purpose of current study.It is clear that classification which combines spatial and spectral details is advantageous in separation different classes, in addition to the use of image enhancements which increases the interpretation. Hereto this has reflected positively to reach high accuracy in classification results. Moreover fusing between two different sensors namely Cosmo-SkyMed with Landsat7 where

the two different methods used include PCS and BT. We have chosen the best of them, depending on the method that gives us more accurate results according quantitative method technique based RMSE. In this paper the classification has been taken advantage of in order to provide us with the required information necessary for decision makers through maximum utilization of multi-sensors; by fusing them to the fullest extent such as spatial and spectral information; by employing them to separate and distinguish different classes than producing a lot of landuse/landcover maps . This paper paves the way to make use of information available from satellite imagery spectral /spatial in areas that suffer from a lack of geo-information. Moreover this paper, including its methodology and alogrithims, can be extrapolated, applied and exported to other areas or datasets.

The Cosmo-SkyMed image with two polarisation, HH and VV, was very effective especialy when fused with Landsat 7. The resulltant image could prove more useful than either image alone in increasing the accuracy of classification. Due to the fact that Object-oriented classifications rely on both the spectral information and the spatial information contained in digital images, it was the best technique to classify fused image. The other classification methods, such as decision tree classification, were used to classify QuickBird image which also gave good results when utilising DTM and NDVI values for the study case.

Aknowledgements

I would like to thank academic staff in Institute for Cartography, TU Dresden for their valuable Support also I would like to thank ‘’e-GEOS, ASI/Telespazio company www.e-geos.it ’’ for providing SAR data free of charge and GIS Unit in Ainkawa, Ministry of Planning, Kurdistan Region ’’ for providing optical data.

References

Aitkenhead M., 2008. A Co-evolving Decision Tree Classification Method. Expert Systems with Applications 34: 18–25.

Aksoy, S., Koperski, K., Tusk, C. and Marchisio, G., 2004. Interactive training of advanced classifiers for mining remote sensing image archives. In Proceedings of the Tenth ACMSIGKDD International Conference on Knowledge Discovery and Data Mining (KDD '04), 22–25 August 2004, Seattle, WA (New York, NY: ACM), pp. 773–282.

Anderson J. R., Hardy E. E., Roach J. T.,and Witmer R. E., 1976. A Land Use and Land Cover Classification System for Use with Remote Sensor Data. Geological Survey Dallas L. Peck Director First Printing 1976.

Ashraf Salman, Brabyn Lars,and Hicks Brendan J.,2012. Image data fusion for the remote sensing of freshwater environments. Applied Geography 32: 619–628.

Baatz M. and Schäpe A., 2000. Multi Resolution Segmentation: an Optimization Approach for High Quality Multi-scale Image Segmentation. Angewandte Geographische Informationsverarbeitung XII. Beiträge zum AGIT Symposium Salzburg, Karlsruhe, Herbert Wichmann Verlag, :12–23.

Benz U.C., Hofmann P.,Willhauck G., Lingenfelder I.,and Heynen M., 2004. Multi-resolution, Object-oriented Fuzzy Analysis of Remote Sensing Data for GIS-ready Information. J Photogramm. Remote Sens. 58: 239–258.

Benediktsson J.A. and Kanellopoulos I., 1999. Classification of multisource and hyperspectral data based on decision fusion. IEEE Transactions on Geoscience and Remote Sensing, 37: 1367–1377.

Bhaskaran S., Paramananda S.,and Ramnarayan M., 2010. Per-pixel and Object-oriented Classification Methods for Mapping Urban Features Using Ikonos Satellite Data. Applied Geography 30: 650–665.

Biro T.K.G., 2011. Geovisualisation of Multi-Temporal Satellite Data for Landuse/Landcover Change Analysis and its Impacts on Soil Properties in Gadarif Region, Sudan. PhD (Dissertation). Dresden University of Technology.

Bouziani M., Goita K., and He D.C., 2010. Automatic Change Detection of Buildings in Urban Environment from Very High Spatial Resolution Images Using Existing Geodatabase and Prior Knowledge. ISPRS Journal of Photogrammetry and Remote Sensing 65 (1): 143–153.

Buchroithner M., 1993. Cartographic Information Extraction from SAR Images Using Filtering and Textural Analysis, SAR Geocoding: Data and Systems. Karlsruhe, Wichmann: 353–372.

Cetin M. and Musaoglu N.,2009. Merging hyperspectral and panchromatic image data: qualitative and quantitative analysis. International Journal of Remote Sensing, 30(7): 1779–1804.

Chavez P. S., Jr., Sides, S. C., and Anderson J. A.,1991. Comparison of three different methods to merge multi-resolution and multispectral data: Landsat TM and SPOT panchromatic. Photogrammetric Engineering & Remote Sensing, 57(3): 295–303.

Dean, A.M. and Smith, G.M., 2003. An Evaluation of Per-parcel Land Cover Mapping Using Maximum Likelihood Class Probabilities. International Journal of Remote Sensing 24: 2905–2920.

Definiens Developer 7- Reference Book, 2007. Definiens AG. Trappentreustr. 1D-80339 Munich, Germany.

Dong J., Zhuang D., Huang Y., and Fu, J.,2009. Advances in multi-sensor data fusion: algorithms and applications. Sensors, 9(10): 7771–7784.

Doxani G., Karantzalos K., and Tsakiri- Strati M., 2012. Monitoring Urban Changes Based on Scale-space Filtering and Object-oriented Classification. International Journal of Applied Earth Observation and Geoinformation 15: 38–48.

ERDAS Field Guide™, 2010. ERDAS, Inc: United States of America.ERDAS Field Guide™, Volume One, United States of America.

ERDAS. (November 2009). ERDAS imagine ver. 9.2 software help document. Norcross, GA: ERDAS Inc.

Gamanya R., De Maeyer P., and De Dapper M., 2007. An Automated Satellite Image Classification Design Using Object-oriented Segmentation Algorithms: A Move Towards Standardization. Expert Systems with Applications 32: 616–624.

Gangkofner U. G., Pradhan P. S., and Holcomb D.W.,2008. Optimizing the high-pass filter addition technique for image fusion. Photogrammetric Engineering & Remote Sensing, 74(9): 1107–1118.

Gnanadurai D., Sadasivam V., Nishandh J.P.T., Muthukumaran L., and Annamalai C.,2009. Undecimated double density wavelet transform based speckle reduction in SAR images: Computers and Electrical Engineering, 35: 209–217.

Goetz S.J., Wright R., Smith A.J., Zinecker E.,and Schaub E., 2003. IKONOS Imagery for Resource Management: Tree Cover, Impervious Surfaces and Riparian Buffer Analyses in the Mid-Atlantic Region. Remote Sensing of Environment 88 (1-2): 195–208.

Gong P.,1994. Integrated analysis of spatial data from multiple sources: an overview.Canadian Journal of Remote Sensing, 20: 349–359.

Herold, M., Scepan, J. (2002). Object-oriented mapping and analysis of urban land use/cover using Ikonos data. In. Proceedings of 22nd EARSEL symposium geoinformation for European-wide integration, Prague, June, 2002.

Jensen, J.R., 1996, Introduction to Digital Image Processing: A remote sensing perspective, 2nd ed. (Piscataway, NJ: Prentice Hall).

Jimenez L.O., Morales-Morell, A. and Creus, A., 1999. Classification of hyperdimensional data based on feature and decision fusion approaches using projection pursuit,majority voting, and neural networks. IEEE Transactions on Geoscience and Remote Sensing, 37: 1360–1366.

Joshi P. K., Roy P. S., Singh S., Agrawal S., and Deepshikha Y.,2006. Vegetation cover mapping in India using multi-temporal IRS Wide Field Sensor (WiFS) data. Remote Sensing of Environment, 103(2):190–202.

Kandrika S. and Roy P.S.,2008. Landuse Landcover Classification of Orissa Using Multi Temporal IRS-P6 AWIFS Data: a Decision Tree Approach. International Journal ofApplied Earth Observation and Geoinformation 10: 186–193.

Landgrebe, D.A., 2003. Signal Theory Methods in Multi-spectral Remote Sensing. Hoboken, NJ: John Wiley and Sons.

Lee J.S., 1986. Speckle Suppression and Analysis for Synthetic Aperture Radar Images. Opt. Eng 25 (5): 636–43.

Lee J.S. and Jurkevich, I., 1990. Coastline Detection and Tracing in SAR Images. IEEE Transactions on Geoscience and Remote Sensing 28(4):662– 8.

Lillesand T.M., Kiefer R.W., and Chipman J.W., 2008. Remote Sensing and Image Interpretation, fifth ed. New York, Wiley.

Li S., Li Z., and Gong J.,2010. Multivariate statistical analysis of measures for assessing the quality of image fusion. International Journal of Image and Data Fusion, 1(1):47– 66.

Li W., Zhang, Q.,and Zhang, Y..2007. Research on the fusion methods with high information preservation. In. Fourth international Conference on Fuzzy Systems and Knowledge Discovery (FSKD 2007), vol. 2 (pp. 487e491). Haikou, China: IEEE.

Lopes A., Touzi R.,and Nezry E.,1990. Adaptive Speckle Filters and Scene Heterogeneity. IEEE Transactions on Geoscience and Remote Sensing 28 (6); 992–1000.

Lopes A., Nezry E., Touzi R.,and Laur H., 1993. Structure Detection and Statistical Adaptive Speckle Filtering in SAR Images. International Journal of Remote Sensing 14: 1735–1758.

Lua Y., Gao Q., Zhang D., andSun D., 2011. Directionlet-based bayesian filter for SAR image despeckling: Procedia Engineering, 15 :2788–2792.

Luo R.C. and Kay M.G., 1989. Multi-sensor integration and fusion for intelligent systems. IEEE Transactions on Systems, Man, and Cybernetics, 19: 901–931.

Lu, D., Weng, Q., 2007. A Survey of Image Classification Methods and Techniques for Improving Classification Performance. International Journal of Remote Sensing 28 (5), 823–870.

Maged M., 2001. Radar Automatic Detection Algorithms for Coastal Oil Spills Pollution. International Journal of Applied Earth Observation and Geoinformation 3 (2): 19 –196.

Mahmoud, A., 2012. Plot-Based Land-Cover and Soil-Moisture Mapping Using X-/L-Band SAR Data: Case Study Pirna-South, Saxony, Germany. PhD (Dissertation). Dresden University of Technology.

Mathieu R, Freeman C.,and Aryal, J., 2007. Mapping Private Gardens in Urban Areas Using Object-oriented Techniques and Very High-resolution Satellite Imagery. Landscape and Urban Planning 81: 179–192.

Navulur K., 2007. Multi-spectral Image Analysis Using the Object-oriented Paradigm. CRC Press, Taylor and Francis Group. Boca Raton London New York.

Nerzy E., Leysen, M.,and De Grandi G., 1995. Speckle and Scene Spatial Statistical Estimators for SAR Image Filtering and Texture Analysis: Some Applications to Agriculture, Forestry, and Point Targets Detection. Proc SPIE 2584: 110–20.

OCHA , UNAMI, 2009. Erbil Governorate Profile. OCHA and UNAMI Participating Agencies and NGOs UNAMI, OCHA, UNDP, UNICEF, UNFPA, FAO, WHO, UNHCR, WFP, ILO, IOM, Mercy Corps. International Medical Corps, GenCap and IMMAP.

Ouyang, Z., Zhang, M., Qi Shen, X., Guo, H., and Zhao, B., 2011. A Comparison of Pixel-based and Object-oriented Approaches to VHR Imagery for Mapping Saltmarsh Plants. Ecological Informatics 6, 136–146.

Ouattara T., Gwyn Q. H. J., and Dubois J.M., 2004. Evaluation of Runoff Potential in High Relief Semi-arid Regions, Using Remote Sensing Data: Application to Bolivia. International Journal of Remote Sensing 2 (25): 423–435.

Pal M. and Mather, P.M., 2003. An Assessment of the Effectiveness of Decision Tree Methods for Landcover Classification. Remote Sens. Environ. 86: 554–565.

Petropoulos G.P., Kalaitzidis C.,and Vadrevu K.P., 2012. Support Vector Machines and Object-based Classification for Obtaining Land-use/cover Cartography from Hyperion Hyperspectral Imagery. Computers and Geosciences 41: 99–107.

Pinho, C.M.D., Silva, F.C., Fonsesa, L.M.G. and Monteiro, A.M.V., 2008. Urban landcover classification from high-resolution images using the C4.5 algorithm. In XXI Congress of the International Society for Photogrammetry and Remote Sensing, 3–11 July 2008, Beijing, China (China: Lu Xiaohong):695–699.

Prechtel N., 2000. Computer-assisted Large Area Landuse Classifications with Optical Remote Sensing. Remote Sensing for Environmental Data in Albania. A Strategy for Integrated Management Nato Science Series, 2. Environmental Security Kluwer, Dordrecht/Boston/London 72: 101–126.

Pradhan P. S., King R. L., Younan N. H., and Holcomb D. W., 2006. Estimation of the number of decomposition levels for a wavelet-based multiresolution multisensory image fusion. IEEE Transactions on Geoscience and Remote Sensing, 44(12): 3674–3686.

Punia M., Joshi P.K.,and Porwal M.C., 2011. Decision Tree Classification of Land Use Landcover for Delhi, India Using IRS-P6 AWiFS data. Expert Systems with Applications 38: 5577– 5583.

Russell S.J.and Norvig P., 2002. Artificial Intelligence, A Modern Approach second ed. Prentice, Hall.

Saha K., Wells N., and Munro-Stasiuk M., 2011. An Object-oriented Approach to Automated Landform Mapping: A case study of drumlins. Computers and Geosciences 37: 1324–1336.

SARMAP, 2007. The SAR Guidebook: Examples Based on SARscape. CREASO.

Sheng, Y., Xia, Z., 1996. A Comprehensive Evaluation of Filters for Radar Speckle Suppression. Proceedings of Geoscience and Remote Sensing Symposium, 1996. IGARSS '96. 'Remote Sensing for a Sustainable Future', May 27–31, Lincoln, Nebraska, USA. IEEE 3, 1559–1561.

Shettigara V. K.,1992. A generalized component substitution technique for spatial enhancement of multispectral images using a higher resolution data set. Photogrammetric Engineering and Remote Sensing, 58(5): 561–567.

Silva, M.P.S., CÂmara, G., Escada, M.I.S. and Souza, R.C.M., 2008. Remote sensing image mining: detecting agents of land use change in tropical forest areas. International Journal of Remote Sensing, 29: 4803–4822.

Stehman S. V.,1996. Estimation of Kappa coefficient and its variance using stratified random sampling. Photogrammetric Engineering and Remote Sensing, 26: 401–407.

Wang X. and Niu R., 2010. Landslide Intelligent Prediction Using Object-oriented Method. Soil Dynamics and Earthquake Engineering 30: 1478–1486.

Wang Z., Ziou D., Armenakis C., Li D., and Li, Q.,2005. A comparative analysis of image fusion methods. IEEE Transactions on Geoscience and Remote Sensing, 43(6): 1391–1402.

Zhang, L., Balz, T., Liao, M., 2012. Satellite SAR Geocoding with Refined RPC Model. ISPRS Journal of Photogrammetry and Remote Sensing 69, 37– 49.